

Assessing the grid impact of Electric Vehicles, Heat Pumps & PV generation in Dutch LV distribution grids

Damianakis, Nikolaos; Mouli, Gautham Ram Chandra; Bauer, Pavol; Yu, Yunhe

DOI

[10.1016/j.apenergy.2023.121878](https://doi.org/10.1016/j.apenergy.2023.121878)

Publication date

2023

Document Version

Final published version

Published in

Applied Energy

Citation (APA)

Damianakis, N., Mouli, G. R. C., Bauer, P., & Yu, Y. (2023). Assessing the grid impact of Electric Vehicles, Heat Pumps & PV generation in Dutch LV distribution grids. *Applied Energy*, 352, Article 121878. <https://doi.org/10.1016/j.apenergy.2023.121878>

Important note

To cite this publication, please use the final published version (if applicable). Please check the document version above.

Copyright

Other than for strictly personal use, it is not permitted to download, forward or distribute the text or part of it, without the consent of the author(s) and/or copyright holder(s), unless the work is under an open content license such as Creative Commons.

Takedown policy

Please contact us and provide details if you believe this document breaches copyrights. We will remove access to the work immediately and investigate your claim.



Assessing the grid impact of Electric Vehicles, Heat Pumps & PV generation in Dutch LV distribution grids[☆]

Nikolaos Damianakis^{*}, Gautham Ram Chandra Mouli, Pavol Bauer, Yunhe Yu

Technische Universiteit Delft (TU Delft), Faculty of Electrical Engineering, Mathematics, and Computer Science, Electrical Sustainable Energy Department, Mekelweg 4, 2628 CD Delft, The Netherlands

ARTICLE INFO

Keywords:

LCT
PVs
EVs
Heat pumps
Distribution grids
Grid impact

ABSTRACT

Low Carbon Technologies (LCTs), such as Photovoltaics (PVs), Electric Vehicles (EVs), and Heat Pumps (HPs), are expected to cause a huge electric load in future distribution grids. This paper investigates the grid impact in terms of over-loading and nodal voltage deviations in different distribution grids due to increasing LCT penetrations. The major objectives are the identification of the most severe LCT, grid impact issue, seasonal effect, and vulnerable distributional area, considering the physical models of the LCTs. It is concluded that Winter is the most hazardous for the future grid impact, characterized by nearly 3 times higher over-loading and 2.5 times higher voltage deviations during high HP penetrations, while suburban areas are the most vulnerable. Moreover, while HPs seem to have, in general, a greater impact compared to EVs, EVs cause more prolonged violations. While this work follows a bottom-up approach, using detailed physical models, aggregated national data has also been acquired, which is often used by top-down approaches. Different grid impact issues have been compared for the two approaches in terms of magnitude and duration. While bottom-up approaches generate more pessimistic results regarding the magnitude of the violations, results about the duration of the violations can be contradictory.

1. Introduction

Due to the ever-growing environmental impact and depletion of fossil fuels, 197 nations, including the Netherlands, have pledged to keep global warming below 1.5 °C until 2050, focusing on decreasing the greenhouse gas emissions during the “Paris Agreement” in 2015 [1]. In this regard, the residential sector alone is responsible for 24–26.7% of the total annual mainly fossil fuel-based energy use in 2010, as found by analysis of 27 European countries (EU-27) [2], while in [3] it has been reported to contribute to 70% of the total carbon emissions. Moreover, the heating and transportation sectors have been defined to be two of the greatest contributors to environmental pollution globally (see Fig. 1). In the Netherlands, the mobility sector accounts for 20% of the total energy demand and comprises mainly Internal Combustion Engine (ICE) based vehicles. Moreover, the highest part of heating in most EU countries is produced by gas-fired boilers (84.2% of households in the UK [4]). Finally, a more recent analysis, published by Eurostat in [5], shows that the transportation sectors and buildings are responsible for 23.2% and 15.4% of the total gas emissions in Europe, respectively.

Considering all of the above, it is obvious that electrification of heating and transportation, as well as sustainable (electric) energy supply, are cornerstones of the success of the global energy transition and world decarbonization. In this regard, Photovoltaics (PVs) on the supply side as well as Heat Pumps (HPs) and Electric Vehicles (EVs) on the demand side, are three of the most significant technologies for the achievement of the aforementioned goals, called “Low-Carbon Technologies” (LCTs).

However, LCTs do not come without the side effect of major grid impact. For example, increased power peaks [1] and load consumption [2] were seen due to energy demand electrification, leading inevitably to grid capacity reduction and congestion in distribution grids [6]. Moreover, power quality issues, such as over-/under-voltage deviations, were reported in [7], while vastly uncertain and rapidly changing PV power caused voltage fluctuations or light flickering in [8]. Additionally, cables and transformers overloading were seen in [9], which could also lead to even more important hazards such as blackouts. Finally, an increase in phase and voltage imbalance was observed due to the connection of single-phase generators (e.g. PVs) or electric loads

[☆] This study is funded by the Dutch Research Council (NWO) as part of the ongoing research project NEON.

^{*} Corresponding author.

E-mail address: n.damianakis@tudelft.nl (N. Damianakis).

Nomenclature

\dot{m}_{wat}	Flow Water Rate of the Heat Pump
\dot{Q}_{cond}	Conduction Losses
\dot{Q}_{hp}	Heat Pump Output
\dot{Q}_{ir}	Heat by Irradiation
\dot{Q}_{los}	Heating Losses
\dot{Q}_{vent}	Ventilation Losses
$\eta^{25\text{ }^\circ\text{C},G^{inc}}$	PV Efficiency under Module Temperature 25 °C and Irradiation G^{inc}
η^{inv}	PV Inverter Efficiency
η^{real}	Real PV Efficiency
$\eta^{T_M,G^{inc}}$	PV Efficiency under Module Temperature T_M and Irradiation G^{inc}
η_{stc}	PV Module efficiency under Standard Test Conditions
ρ_{air}	Air Density
θ_M	Tilt angle of the PV Module
θ_s	Angle of Solar Elevation
A_M	Module Area
af	Absorptivity Factor
AOI	Angle of Solar Incidence
Az_M	Azimuth of the PV Module
Az_s	Azimuth of the Sun
B_{ev}	Battery Capacity of the EV
c_η	Temperature Coefficient of PV Efficiency
C_{air}	Air specific Capacity
C_b	Building Thermal Capacity
$c_{P_{MPP}}$	Temperature Coefficient of Maximum Power Point PV Power
C_{wat}	Water specific Capacity
E_r	Requested Energy of the EV
FF	Fill Factor of PV Module
G_{inc}	Incident Irradiation
G_{noct}	Incident Irradiation under Normal Operation Conditions
$I_{SC}^{25\text{ }^\circ\text{C},G^{stc}}$	PV Module Short-circuit Current under Module Temperature 25 °C and Irradiation G^{inc}
I_{ch}	EV Charging Current
I_{cv}	Constant-Voltage Region Charging Current
I_r	Rated EV Charging Current
$P_{MPP}^{25\text{ }^\circ\text{C},G^{inc}}$	Maximum Power Point PV Power under Module Temperature 25 °C and Irradiation G^{inc}
P_{hp}^r	HP Rated Power
P_{PV}^r	PV Rooftop Rated Power
P_{MPP}^{stc}	Maximum Power Point PV Power under Standard Test Conditions
$P_{MPP}^{T_M,G^{stc}}$	Maximum Power Point PV Power under Module Temperature T_M and Irradiation under Standard Test Conditions
P_{hp}	Heat Pump Power Consumption
P_{pv}	PV Power Generation
s_w	Wind speed
SOC	State of Charge of the EV
T_a	Ambient Temperature

T_b	Building Temperature
T_M	PV Module Temperature
T_{noct}	Temperature of the PV Module under Normal Operation Conditions
T_{ret}	Return Water Temperature of the Heat Pump
T_{sup}	Supply Water Temperature of the Heat Pump
$V_{OC}^{25\text{ }^\circ\text{C},G^{stc}}$	PV Module Open-circuit Voltage under Module Temperature 25 °C and Irradiation G^{inc}
V_b	Building Volume

Abbreviations

AC	Alternate Current
ASHP	Air-sourced Heat Pump
CC	Constant Current (Charging Region)
COP	Coefficient of Performance
CV	Constant Voltage (Charging Region)
DA	Distributional Area
DC	Direct Current
DHW	Domestic Hot Water
DMP	Duration-Magnitude Product
EV	Electric Vehicle
HP	Heat Pump
LCT	Low-Carbon Technology
LV	Low Voltage
MCS	Monte-Carlo Simulation
MPP	Maximum Power Point
MV	Medium Voltage
NOCT	Normal Operation (PV) Cell Temperature
O-C	Open Circuit
O/L	Overloading
OV-UV	Overvoltage-Undervoltage
PV	Photovoltaics
S-C	Short-Circuit
STC	Standard Test Conditions
T/F	Transformer

(e.g. EVs) in distribution grids [10,11]. All of the above constitute important issues, which prove that successful 100% integration of LCTs cannot be achieved unless the challenges mentioned above are managed.

2. Literature overview & contributions

2.1. Grid impact of PVs-EVs penetrations

The vast majority of the state-of-the-art research on the grid impact of combined LCTs investigates the PVs-EVs combination. For example, the authors in [8] investigated how increasing penetrations of photovoltaic generation and EVs affect voltage issues and fluctuations, while their effect on phase imbalance has been studied in [11–13]. Moreover, transformer overloading was found to be the worst issue in rural distribution grids, starting with 109% even from 25% penetration of PVs-EVs in [14]. On the contrary, undervoltage violations started first, especially for longer feeders at 40% penetration of PVs-EVs in [15]. Furthermore, PV integration was more closely connected to voltage violations (1.79 p.u. overvoltage even from 15% penetration), while EVs provoked mainly cable over-loading in [16]. Different

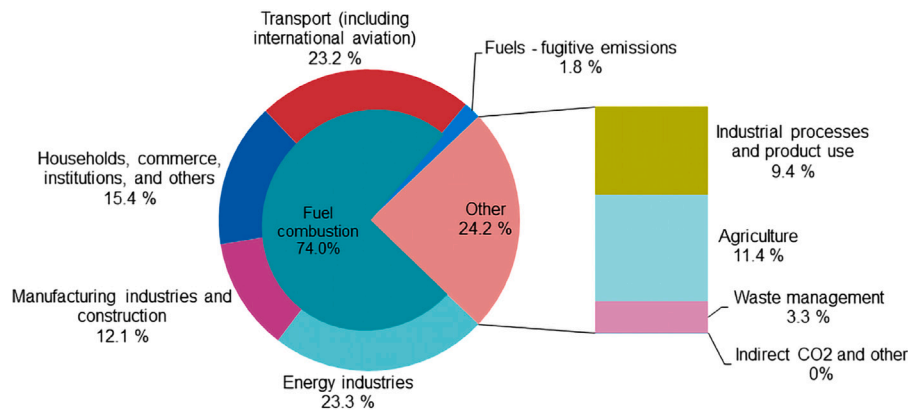


Fig. 1. Greenhouse gas emissions by source sector, EU, 2020 (Eurostat [5]).

combinations of EV and PV penetrations showed a general trend for residual load peaks at 15:00, while peak load demands due to charging appeared at 19:00 in [17]. Finally, harmonic distortion from various increasing EV & PV combinations is also studied in [18] & [19]. The impact of co-integration of EVs & PVs as well as potential solutions have also been studied in [20,21]. In [20], individual and combined EV & PV penetrations have been investigated in a real metropolitan area in Arizona, however, only peak hour demand and consumption were analyzed. On the contrary, in [21], the analysis also comprised voltage deviations and system power losses, however, the investigation remained in the IEEE European LV Test Feeder.

2.2. Grid impact of HPs-EVs penetrations

The Grid Impact of HPs-EVs has also been studied in the literature. Load profiles of a variety of rural grids have been analyzed in [22] under increasing EV and HP penetrations. Moreover, EVs had a higher impact on unbalance in [23], while HPs were found to provoke loading violations from lower penetrations (from 40%) in [24]. In [25], EV slow- and fast-charging scenarios together with HP use have been analyzed for a zero-energy dwelling, where power peaks increased up to 155%, especially in the fast-charging integrated scenarios. The effect of different load approaches, HPs-EVs penetrations, and real grid areas on various grid impact issues, such as loading utilization and voltage deviations, has been studied in [7]. Furthermore, no voltage violations or cable overloading were seen in the urban grids of [4] in most cases constructed with individual or combined increasing EV & HP penetrations, apart from transformer overloading during the extreme winter scenario in 2050. Authors in [26] also incorporated coordination strategies for grid impact minimization, finding that without coordination, high grid investments will be needed for hosting EV charging and HP operation, simultaneously. However, the analysis remained in a standard distribution network and comprised only voltage deviations and control.

2.3. Grid impact of PVs-HPs penetrations

Some works are also devoted to studying HP and PV integration in distribution. Authors in [27] calculated the grid reinforcement needed for various PVs-HPs penetration scenarios finding that in rural grids, HPs integration will lead to higher reinforcement cost than PV. Rural feeders seemed to be also vulnerable to overloading and undervoltage in [3], while cable overloading was expected even from 30% LCT penetrations. Transformer overloading was also found to be crucial in [28], reaching up to 240% for 100% PV-HP penetrations, whereas the required grid capacity was found to be 3 times higher in [29]. Finally, weather and seasonal effects were also investigated in [30], while the decrease of the identified grid impact with the use of batteries

and higher insulation was also studied in [31]. However, the analysis in [31] remained only on the electricity load profiles of residential areas.

2.4. Grid impact of PVs-EVs-HPs penetrations

While the impact of the previous individual LCT pairs has been investigated in-extent, a few works have investigated the impact of all 3 technologies (PVs, EVs, and HPs) together.

The impact of the 3 LCTs on household-level load profiles was investigated in [32], where EVs were found to be the “heaviest” LCT, contributing to 4.7 times higher power peaks and 13 times more peak hours. However, the impact on load profiles was analyzed only individually for each LCT. On the contrary, the impact of combined and individual PVs-EVs-HPs integration on the future load profiles (energy consumption & peak power demand) has been analyzed in [1] & [2] for the country of Switzerland and a residential hypothetical Dutch LV network, respectively. Furthermore, the overloading of components has been studied in [33], where EVs were found to have the highest impact on transformer loading. Authors in [34] also studied the overloading impact, however, they considered only the combined penetrations of the 3 LCTs. Hence, this analysis cannot provide insights into the contribution of every LCT to the overall grid impact.

All of the previous works have analyzed only one aspect of the overall future grid impact. A comparison of voltage violations and overloading issues was performed under the increase of different LCTs in [6] & [35], where it was found that the older Dutch generation networks cannot sufficiently host the future load demand. Energy losses and power factors were also encapsulated in the analysis of [36]. The authors in [37] also investigated the impact on harmonics and unbalance, where PVs & HPs were more linked to voltage variations and harmonics. Furthermore, the effect of different LCT penetrations on the load profiles and voltage variations for the Irish distribution network was studied in [38], however, this effect was investigated only in combined integration.

All of the previous works either use only one standard/adapted or a real LV network for their investigation, leaving out the effect of the different grid case studies on the grid impact assessment results. In [9] & [39], 25 and 5 UK LV networks were used to study the impact of different future LCT penetrations on load profiles, voltage violations, and overloading. In [9], PV integration was more connected to voltage violations (from 30% penetration). However, LCT integration was studied only individually in [9], whereas it was studied only in combination in [39]. While these works used multiple grids for the grid impact assessment, they did not distinguish their grids into different categories (grid areas), in order to observe how characteristics from different grid areas affect the grid impact results. Different sectors of interest (e.g. residential or commercial) and different population areas

Table 1
Characteristics of existing grid-impact assessment works with PVs-EVs-HPs consideration.

Ref	Grids (Type & No.)	Impact issues	Penetrations (C. and/or I.)	LCT comparison	top-down	bottom-up
[32]	German Household	LP	1 (I)	✓		✓(simp)
[1]	Switzerland	LP	Multiple (C & I)	✓	✓	
[2]	1 hypothetical Dutch LV Grid	LP	Multiple (C & I)	✓		✓
[33]	1 Brescia MV Grid	O/L	1 (C & I)	✓	✓	
[34]	1 Dutch LV Grid	O/L	Multiple (C)		✓	
[6]	1 Swiss LV Grid	O/L, V	Multiple (C & I)			✓(simp)
[35]	2 Dutch LV Grids (old, new)	O/L, V	1 (C)		✓	
[36]	1 adapted LV Grid	V, U, PF, EL	1 (C & I)	✓		✓(simp)
[37]	1 UK LV Grid	O/L, V, U, H	1 (I)	✓	✓	
[38]	1 Irish Grid	LP, V	Multiple (C)		✓	
[9]	25 UK residential LV Grids	LP, O/L, V	Multiple (I)	✓	✓	
[39]	5 UK LV Grids	LP, O/L, V	Multiple (C)		✓	
[40]	UK Rur, Suburb, Urb Grids	LP	1 (C & I)	✓	✓	
[41]	Rur, Suburb, Urb Grids	O/L, V	1 (C)		✓	
[42]	2 Munich Grids (Suburb, Urb)	LP	Multiple (I)	✓	PVs, EVs	HPs
This Work	6 Dutch Rur, Suburb, Urb Grids	LP, O/L, V	Multiple (C & I)	✓	✓	✓

(e.g. rural–suburban–urban) in [40,41], and [42]. The different grid characteristics played an important role on [42], where only in the urban area EVs & HPs provoked an impact of a similar magnitude. However, the authors in [40] & [42] analyzed only the future load profiles, while in [41] only one penetration of combined LCT integration was studied.

However, all of these works, apart from [2,6] & [36] & [32], constitute “top-down” approaches, using aggregated high-scale data extrapolated to the needed level. On the contrary, bottom-up approaches use physical models to generate the data needed. The target of the bottom-up approaches is to consider the component-side point of view and their physical operation models, aiming for higher validity of results. For example, an EV charging model can incorporate the Constant Current–Constant Voltage (CC–CV) charging region of the EV battery. Additionally, an HP heating model can integrate the buildings’ isolation and, directly, the weather effect on the HPs’ Coefficient of Performance (COP). Moreover, for that reason, they can be highly extendable and modifiable to incorporate different technologies or characteristics of different case studies (e.g. different regions, seasons, etc.) [31]. From the bottom-up approaches, only authors in [2] consider detailed models of the LCTs, whereas the generation of the LCT profiles in [6] & [36] & [32] is mostly performed with the use of 1 or 2 simple regression formulas.

A comparison of the investigation characteristics for every existing work that studies all 3 LCTs (PVs, HPs, EVs) is summarized in Table 1. In Table 1, the following abbreviations stand for:

- For Grids: Rur for Rural, Suburb for Suburban, Urb for Urban.
- For Impact Issues: LP for Load Profiles (Energy Consumption, Peak Power Demand), O/L for Overloading, V for Voltage Deviations, U for Unbalance, PF for Power Factor, EL for Energy Losses, H for Harmonics.
- For Penetrations: C for Combined, I for Individual.
- For Bottom-up: simp for simplistic.

Considering all of the above, a bottom-up investigation is needed that aims to investigate the future grid impact by different individual and combined penetrations of PVs, EVs & HPs, considering multiple grid impact issues and metrics. Hence, insights will be provided about the overall future grid impact, the contribution of each LCT according to each penetration, and the severity of the different issues that should be expected. Moreover, the use of real-world grids with different characteristics is needed so that the effect of the different grid case studies specifications (rural, suburban, urban) is considered on the future grid impact. This has not yet been done with the use of a bottom-up approach. Following a detailed bottom-up approach, the physical models and the realistic operation of the integrated components will be thoroughly considered as well as the different effects that affect them.

For example, the use of different weather data has a direct impact on the COP and power consumption of the HPS, and therefore, the seasonal effect can be taken into account. However, it must be noted that the top-down approaches have the strength of providing high accuracy with low modeling complexity if a lot of historical data is available. In contrast, the validity of the bottom-up approaches is subject to the right selection of appropriate parameters of the utilized models [31,43]. Therefore, the analysis of this work has been repeated, following a top-down approach, so that, firstly, the two approaches are cross-validated, and secondly, important insights are drawn about the impact of the approach on the results. According to the authors’ knowledge, this is investigated for the first time in grid impact studies, concerning LCTs. In this regard, the contributions of this work can be summarized as:

- Analysis of the grid impact in different real Dutch LV residential & commercial distribution grids (urban, suburban & rural), considering in detail the characteristics of the LCT physical models (bottom-up approach).
- Use of multiple metrics to assess several grid impact issues (node voltage deviations and overloading of network components) of individual and combined integration of PVs, HPs & EVs, considering spatial, intra-week & seasonal effects, penetration levels, and existing loading conditions. Hence, the bottom-up grid impact assessment is consistent and thorough with respect to other bottom-up existing works.
- Compares the results mentioned above, generated by physical models (bottom-up) with related results by aggregated data utilization from open-source data sources (top-down) in order to cross-validate the two main grid impact assessment approaches. According to the authors’ knowledge, this has not yet been done in grid impact studies.

The rest of this work is divided as follows: Section 3 comprises the utilized data, models, and methodology, while Section 4 contains the simulation set-up and the work’s case studies. Sections 5 and 6 integrate the results and discussion, respectively. and Section 7 concludes the work.

3. Data description & models of LCTs

In this section, firstly, the utilized data is analyzed and, secondly, the 3 LCT models are explained. In this work, special focus has been placed on the character of the models that should be used for this bottom-up approach. Black-box models are usually suitable for data-driven approaches that have a lot of historical data available. However, they lack of interpretability of results and the various effects that can have an impact on them. On the contrary, white-box models are fundamentally based on the conservation of mass and energy and,

therefore, they are especially suited for bottom-up approaches, because they are able to consider various details of the models. However, this comes at the cost of high computational expense, especially for grid-level studies that comprise hundreds of loads [44]. Hence, the use of grey-box modeling has been decided for the scope of this work, which provides a trade-off between accuracy and computational expense, that suits best a grid-level bottom-up approach.

3.1. Data description

The following data have been used as inputs for the developed models of the bottom-up approach and/or for the extraction of the top-down results:

(1) Dutch electricity distribution consumption profiles of the year 2021 for the already existing electric demand of residential and commercial buildings have been acquired from [45]: used in both bottom-up and top-down approaches.

(2) Probabilistic distributions of EVs, in terms of arrival and departure times, connection times & requested amounts of energy, have been acquired by the Elaad open database [46]: used in both bottom-up (EV model) and top-down approaches. The EV model, however, also comprises more features, explained in Section 3.2.

(3) Weather data (wind speed, ambient temperature, irradiance components, solar elevation & solar orientation profiles) have been acquired from the Meteoronorm database¹: used in bottom-up as input for the PV model (Section 3.4).

(4) Heating data (Space/water heating and COP profiles of various types of Heat Pumps), scaled to total yearly consumption, have been acquired from the When2heat database²: used for the top-down approach results.

(5) PV power distribution profiles scaled to rated power have been acquired from the Royal Dutch Meteorological Institute (KNMI)³: used for the top-down approach results.

3.2. EV model

Using Monte-Carlo Simulation (MCS), 200 weekly profiles are created for 3 different chargers locations (Home, Semi-Public & Public) and randomly distributed to the chargers in grid simulation. The EV pool comprises the “Kona, I3, I-Pace, and Model 3” EVs with rated power of 11 kW, the “Model X, Model S” EVs of 16 kW, and the “Zoe” EV of 22 kW. It is assumed that all AC chargers can provide the maximum power of 22 kW. The Home Chargers, in comparison with Semi-public and Public chargers, are typically characterized by lower EV frequency and higher requested amounts of energy (see Fig. 2). Intra-week effects (weekdays and weekends) have also been taken into account regarding the charging times. For example, an EV is charged 3 times during weekdays and once during weekends at a Home Charger.

Considering the realistic operation of EV charging, also the CC-CV charging region has been considered, utilizing a linear approximation, dictated by (1). EVs are charged at constant rated current I_r until the State-of-Charge (SOC) reaches 80%, where the CV region begins. During the CV region, the charging current decreases linearly to zero until SOC reaches 100%.

$$I_{cv}(t) = 5(1 - SOC(t))I_r(t) \quad (1)$$

$$I_{ch}(t) = \min(I_r(t), I_{cv}(t))$$

Where I_{cv} , I_r & I_{ch} the CV-region, rated & charging currents for every time instant t [47].

This model has also considered a 30% higher consumption for EV charging during the Winter period in order to encapsulate also the

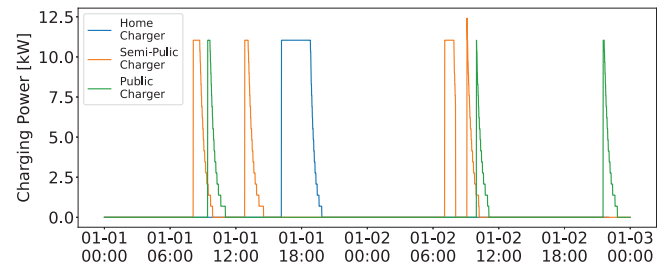


Fig. 2. Typical EV Charging Profiles of Home, Semi-Public & Public Chargers (2 days duration).

seasonal effect. The reason for this consideration is twofold. Firstly, it has been found by data analysis from 7500 EVs, that EV consumption is higher during the Summer than in Winter, due to a number of reasons, e.g lower average temperature change to achieve thermal comfort inside the EV, capability of pre-cooling while plugged in, higher tire pressure, battery operation closer to their comfort zone, etc. [48]. Secondly, the particular investigation takes place in the Netherlands, which is characterized by more moderate Summers than Winters. This difference, regarding the deviation between the ambient and the EV interior temperature, has a direct impact on the cooling and heating COPs and hence, on the power consumption [49]. The 30% increase has been integrated into the arrival SOC of the EVs at the chargers and the related requested energy in (2), assuming that the EV drivers will still request the same SOC upon departure.

$$SOC_{ar}^{win} = 1.3SOC_{ar}^{sum} - 0.3SOC_{dep} \quad (2)$$

$$E_r^{win} = (SOC_{dep} - SOC_{ar}^{win})B_{ev}$$

Where: SOC_{ar}^{win} & E_r^{win} the arrival SOC & requested energy during winter, respectively, SOC_{ar}^{sum} the arrival SOC during summer, B_{ev} the battery capacity of every EV and SOC_{dep} its departure SOC.

3.3. HP & Building models

The HP and building models that are used in this work are based on [49], where a power consumption and building temperature simulator has been designed. The simulator considers space-heating with floor-heating and domestic hot water (DHW) by air-sourced HPs (ASHPs) at residential and commercial buildings. It is fed with building occupancy profiles, HP and building specifications, the insulation model & weather data. The simulator extracts the HP consumption, keeping the space temperature on the desired levels (21°, 23°) when the buildings are occupied. 200 randomized HP residential and commercial consumption profiles have been created with HP-rated power $P_{hp}^r = 3$ kW, modifying the building occupancy profiles, and randomly integrated into grid simulation. For example, the hours that people leave and return to residential buildings (08:00 & 14:00, respectively) have been replaced by normal distributions at 07:45 & 14:45, respectively.

$$T_b(t + \Delta t) = \frac{\dot{Q}_{hp}(t) + \dot{Q}_{ir}(t) - \dot{Q}_{los}(t)}{C_b + V_b C_{air} \rho_{air}} \Delta t + T_b(t) \quad (3)$$

where:

$$\dot{Q}_{los}(t) = \dot{Q}_{cond}(t) + \dot{Q}_{vent}(t) \quad (4)$$

Eq. (3) dictates the temperature of the building T_b at every timestep Δt , which depends on the total heat input of the building (HP output \dot{Q}_{hp} & heat from incident solar irradiation \dot{Q}_{ir}), the total building losses \dot{Q}_{los} (conductive losses \dot{Q}_{cond} & ventilation losses \dot{Q}_{vent}) and the total heating capacity (building capacity C_b and capacity of the air volume inside the building V_b).

$$P_{hp}(t) = \frac{\dot{Q}_{hp}(t)}{COP(t)} \quad (5)$$

¹ <https://meteonorm.com/>

² <https://data.open-power-system-data.org/when2heat/>

³ <https://www.knmi.nl/>

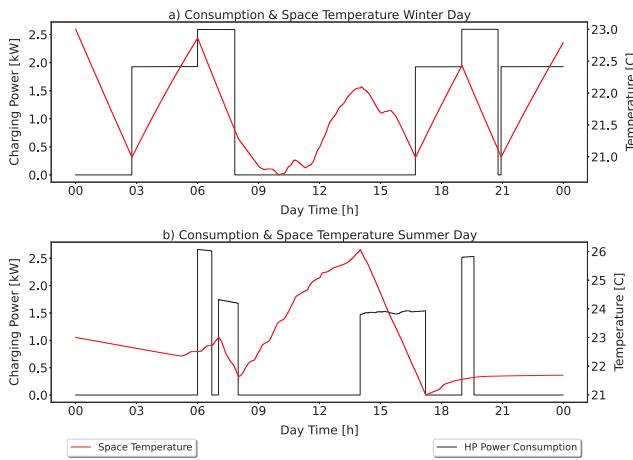


Fig. 3. Power Consumption & Space Temperature at Residential Buildings.

Table 2

Parameters of HP & Building models.

Parameters	Explanation	Value
C_b	Building Thermal Capacity	4.755 kWh/K
V_b	Building Volume	585 m ³
C_{air}	Air Specific Capacity	0.279 Wh/kgK
ρ_{air}	Air Density	1.225 kg/m ³
\dot{m}_{wat}	HP Flow Water Rate	0.8 kg/s
C_{wat}	Water Specific Capacity	1.16 Wh/kgK
P_{hp}^r	HP Rated Power	3 kW

$$COP(t) = 7.90471e^{-0.024(T_{ret}(t)-T_a)} \quad (6)$$

$$T_{ret}(t) = T_{sup} - \frac{\dot{Q}_{hp}(t)}{\dot{m}_{wat} C_{wat}} \quad (7)$$

The HP power consumption is calculated by (5), which dictates its relation to the HP output and COP [4]. The COP and return water temperature T_{ret} are modeled in (6) and (7), where \dot{m}_{wat} : the flow water rate and T_{sup} the supply water temperature, which is set at 35°, 50° and 18° for floor-heating, DHW and floor-cooling, respectively.

In Fig. 3, the HP consumption and the building temperature are depicted during heating mode (winter day) & cooling mode (summer day). The space temperature is always within the desired levels (21°–23°), except for the time period that the building is not occupied (from 08:00 until 14:00). The high and low power peaks represent the DHW and space-heating (cooling) modes, respectively.

The parameters of the utilized HP & Building models are summarized in Table 2.

3.4. PV model

Eqs. (8)–(15) dictate the PV model, based on [50].

$$\cos(AOI(t)) = \cos(\theta_M) \sin(\theta_s(t)) + \sin(\theta_M) \cos(\theta_s(t)) \cos(Az_M - Az_s(t)) \quad (8)$$

$$T_M(t) = T_a(t) + \frac{G_{inc}(t)}{G_{noct}} (T_{noct} - 20) \frac{9.5}{5.7 + 3.8s_w} (1 - \frac{\eta_{stc}}{af}) \quad (9)$$

$$P_{MPP}^{T_M, G_{stc}} = P_{MPP}^{stc} + c_{P_{MPP}} (T_M - T_a) \quad (10)$$

$$\eta^{T_M, G_{stc}} = \frac{P_{MPP}^{T_M, G_{stc}}}{A_M G_{stc}} \quad (11)$$

$$P_{MPP}^{25^\circ C, G_{inc}} = FF V_{OC}^{25^\circ C, G_{inc}} I_{SC}^{25^\circ C, G_{inc}} \quad (12)$$

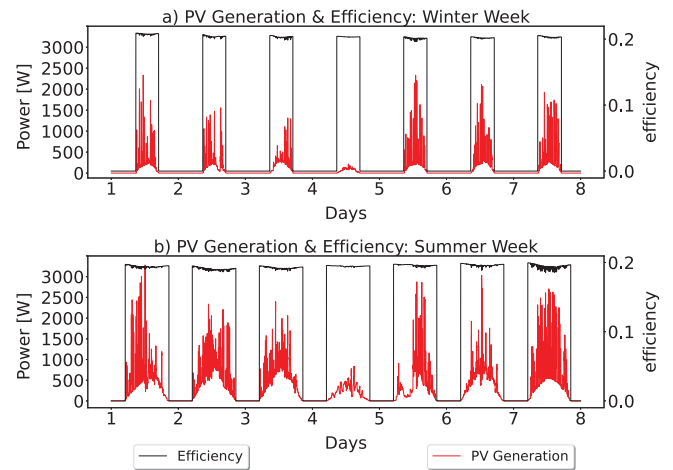


Fig. 4. PV Rooftop 3 kW-rated Power & efficiency for (a) Winter & (b) Summer (tilt angle = 30°, azimuth = 180°).

$$\eta^{25^\circ C, G_{inc}} = \frac{P_{MPP}^{25^\circ C, G_{inc}}}{A_M G_{inc}} \quad (13)$$

$$\eta^{real} = \eta^{25^\circ C, G_{inc}} [1 + \frac{c_\eta}{\eta^{stc}} (T_M - 25^\circ C)] \quad (14)$$

$$P_{pv}(t) = \eta^{real} A_M G_{inc} \eta^{inv} \quad (15)$$

Eq. (8) models the angle of solar incidence (AOI), where θ_M & Az_M the title angle and orientation (azimuth) of the surface and $\theta_s(t)$ & $Az_s(t)$ the momentary solar elevation angle and orientation. It must be noted that the “Isotropic Sky Model” has been utilized for the calculation of diffuse irradiation, and potential shading by other buildings has been neglected. The temperature of the PV model depends on the ambient temperature T_a , the wind speed s_w , the incident irradiance G_{inc} , consisting of the direct, diffuse, and albedo components, the irradiance and temperature under normal operating conditions G_{noct} & T_{noct} , the absorptivity factor af and is estimated by (9).

The effect of the module temperature on the PV power and efficiency is dictated by (10) & (11), where G_{stc} the irradiance under standard test conditions (STC), A_M the module area and $c_{P_{MPP}}$ the power temperature coefficient. Eqs. (12) & (13) dictate the related effect of irradiance on the power of the maximum power point (MPP) and the module efficiency, where FF the module fill factor and $V_{OC}^{25^\circ C, G_{stc}}$ & $I_{SC}^{25^\circ C, G_{stc}}$: the open-circuit (O-C) voltage and short-circuit (S-C) current of the module under different incident irradiance. The real module efficiency, dependent on both incident irradiance and module temperature, and the final PV generation are modeled in (14) & (15), respectively, where η^{inv} the efficiency of the inverter and c_η the power temperature coefficient.

Using MCS, 90 Summer and Winter PV generation profiles have been created using a tilt angle from 10° to 50° with a step of 10° and using an orientation from 0° to 340° with a step of 20°. The profiles are created to represent the various roofs’ orientations in a distribution grid and are, therefore, randomly distributed to the buildings in the grid simulation. All PV rooftops comprise 12 PV panels of MPP power P_{MPP}^{stc} , there all have a rated power $P_{PV}^r = 3$ kW.

Fig. 4 depicts the weekly PV rooftop generation profile and module efficiency during Winter and Summer seasons for the case of 30° tilt angle and 180° azimuth.

The parameters of the utilized PV model are summarized in Table 3.

4. Description of set-up & Case studies

This section contains the description of the distribution grids, the simulation set-up & the definition of the formed case studies and scenarios.

Table 3
Parameters of PV model.

Parameters	Explanation	Value
G_{noct}	Irradiance (NOCT)	800 W/m ²
T_{noct}	Temperature (NOCT)	44 °C
η_{stc}	Efficiency (STC)	0.1943
af	Absorptivity Factor	0.9
P_{MPP}^{stc}	MPP PV Power (STC)	245 W
c_{PMPP}	Power Temp. Coefficient	-0.29 %/°C
G^{stc}	Irradiance (STC)	1000 W/m ²
FF	Fill Factor	0.7888
A_M	Module Area	1.26 m ²
η^{inv}	PV Inverter Efficiency	0.95
$V_{OC}^{25\text{ }^\circ\text{C}, G^{stc}}$	O-C Voltage (25 °C, G^{stc})	53 V
$I_{SC}^{25\text{ }^\circ\text{C}, G^{stc}}$	S-C Current (25 °C, G^{stc})	5.86 A

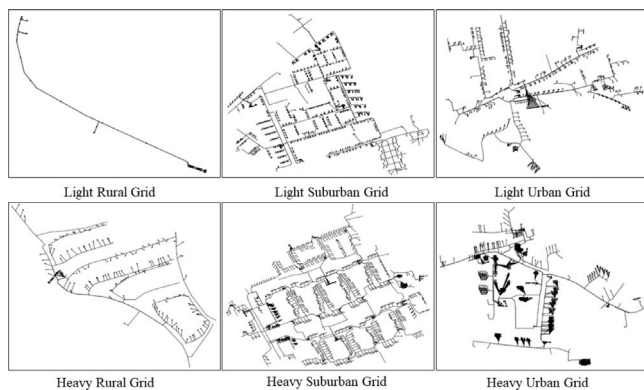


Fig. 5. 6 Dutch LV Distribution Grids, provided by Enexis Groep.

Table 4
Characteristics of distribution grids.

Distribution grids	Nodes	Buildings	Homes
Rural (light-loaded)	23	3	0
Rural (heavy-loaded)	373	138	133
Suburban (light-loaded)	1742	809	772
Suburban (heavy-loaded)	1920	885	809
Urban (light-loaded)	1334	349	269
Urban (heavy-loaded)	1322	876	680

4.1. Investigated distribution grids

As already mentioned, real Dutch distribution grids have been acquired from Enexis Groep⁴ for the purpose of this work. The first 6 distribution grids, 2 for each of the urban, suburban, and rural areas, are low-voltage (LV) comprising residential and commercial buildings. The rationality behind this selection is firstly to investigate different grid topologies and secondly to study representative light-loaded and heavy-loaded distribution grids. Table 4 summarizes the basic grid characteristics: Nodes, Buildings & Homes (residential buildings), while Fig. 5 depicts their spatial visualizations.

4.2. Case studies

The main objective is the thorough identification and quantification of the future grid impact, encapsulating the effects of different distributional grids, LCT conditions, LCT penetrations, seasons, and approaches. In this regard, Table 5 summarizes the developed case studies for the grid impact evaluation.

With the use of the aforementioned case studies, the work intends to identify quantitatively:

- the most vulnerable distributional area according to each selected grid impact metric.
- the most crucial grid impact issue.
- the most “heavy” LCT considering different penetrations.
- the most “heavy” season.
- the total future grid impact of all LCTs integration.

However, the authors acknowledge that grid impact assessment studies are highly dependent on the investigated grid specifications and case study characteristics. Therefore, the results should not be straightforwardly generalized for all case studies, that investigate different distribution grids. Nevertheless, since the investigated grids are provided as area-specific representatives by the Dutch grid operator “Enexis Groep”, this work can provide valuable insights, especially in the case of the Netherlands.

4.3. Simulation set-up

The simulation time period has been selected to be 1 week in order to capture the intra-weekly effects. For example, the heating demand of buildings as well as EV driving and consequently charging behavior, differ greatly during weekdays and weekends and must also be considered. According to the data used for EV charging, drivers tend to charge their EVs 3 times during the week and once during the weekend [46]. Moreover, commercial buildings are less occupied during the weekends, while the opposite applies to residential buildings.

Moreover, the timestep of the simulation has been set to be 1 min. While this timestep can increase the computational expense of the simulation, it provides higher accuracy to the grid impact assessment results. This is particularly important for the consideration of the coincidence of the operation of the different LCTs [7]. Additionally, the durations of the simulations are maintained for every grid case study between 20’ (light rural grid) and 90’ (heavy suburban grid). These durations are appropriate for grid impact assessment studies, that serve scheduling purposes. Finally, the identified grid impact is aimed to be minimized with coordinated power control in future work, where the 1-minute resolution is highly important.

The LCTs are randomly distributed within the grids, and they increase from 0 to 100% simultaneously. Initially, the residential and commercial buildings of every grid and their nodes were identified. Consequently, PVs and HPs were distributed to the buildings, according to the case study penetration. Hence, 100% PV or HP penetration means that every building owns a PV or HP. The EV chargers were also distributed according to the penetration and the number of buildings. However, Home chargers were placed at nodes with residential buildings, while Semi-public and Public chargers were placed at the rest of the nodes. From these nodes, priority was given to the nodes, where commercial buildings were connected. All distributed LCT profiles, within the grids, were randomly chosen with uniform probability function in the Python environment from their respective profile families. The top-down approach uses the data described in Section 3.1., while the bottom-up approach uses the models of Sections 3.2–3.4.

It must be noted that the LCT distributions in every case study are independent of one another, meaning that a building may own a PV rooftop and not an EV or an HP and vice versa. Moreover, every penetration is built on the previous one, meaning that the buildings that owned an HP at 50% penetration will also own an HP at 80% penetration. Furthermore, PV generation and base load are integrated into every LCT condition, therefore, only HPs and EVs have been considered individually and in combination. Hence, LCT conditions can also be called “HP/EV/HP-EV loading conditions”.

Finally, the grid simulation has been performed in the DigSilent PowerFactory 2019 environment with the use of the AC-balanced Newton–Raphson load flow calculation method [51]. This is because

⁴ <https://www.enexisgroep.nl/>

Table 5
Case studies for grid impact evaluation.

Grids	Case studies			Approaches
	LCT conditions	LCT penetrations	Seasons	
2 Rural (light & heavy)	PVs-EVs	0%	Summer	bottom-up
2 Suburban (light & heavy)	PVs-HPs	50%	Winter	top-down
2 Urban (light & heavy)	PVs-EVs-HPs	80%		
		100%		

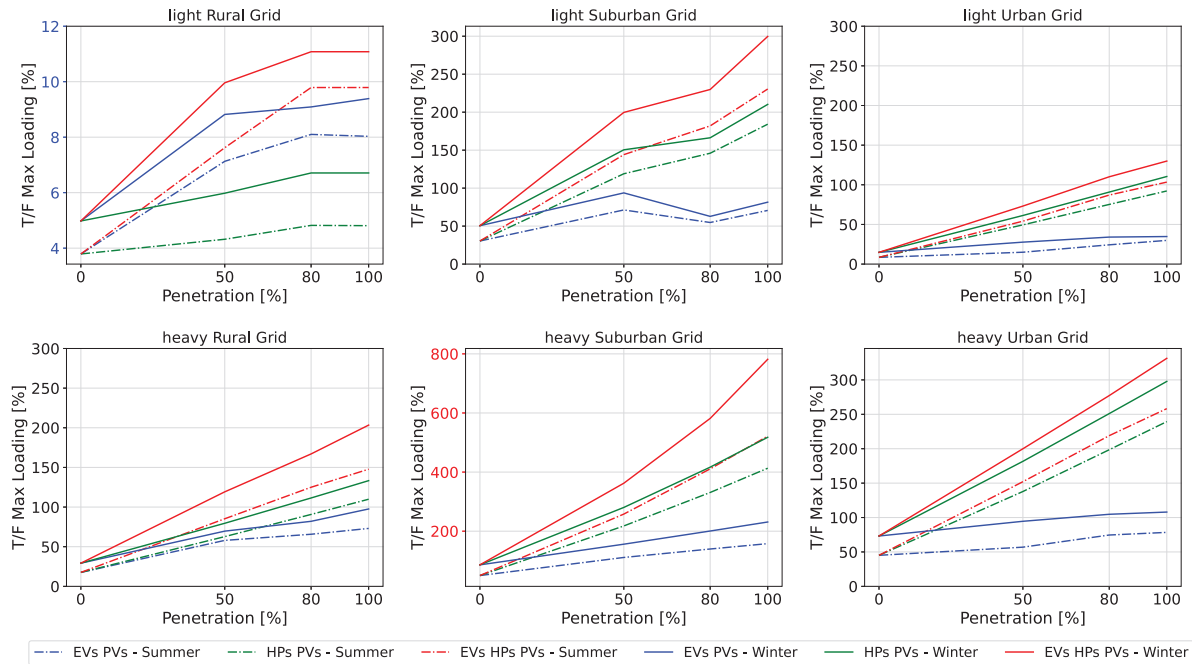


Fig. 6. Total Transformer Maximum Loading per LCT penetration under different LCT conditions and seasons.

the imbalance impact of the LCTs is out of the scope of this work, however, it is intended for future work. The grid simulation has been managed with the use of the Python 3.9 environment.

5. Results & discussion

5.1. Results overview

The grid impact is addressed in all case studies at the following grid components' issues:

- Transformer (T/F) Overloading (O/L) [%].
- Lines Overloading [%].
- Nodes Voltage Deviations (under- and over-voltage) [p.u].

The utilized grid impact metrics for every component are summarized as follows:

- Total (weekly) maximum issue magnitude.
- Total (weekly) issue duration of all violation incidents.
- Total (weekly) issue incidents.
- Magnitude & duration per issue incident.
- (Duration)x(Magnitude) called as Duration-Magnitude Product (DMP) per issue incident: New metric that intends to encapsulate both important aspects of the issue, also defined as "issue's violated area".
- number of simultaneous issue locations within the grid (applies for the lines and the nodes).

5.2. Transformer (T/F) overloading

In Fig. 6, the maximum T/F loading at each distributional grid, for 0%–100% penetrations of the 3 different LCT conditions and 2 seasons, is depicted. Light rural grid is the only distributional area with no violation under every case. On the contrary, the heavy rural grid's T/F is already overloaded at 50% penetration of combined PVs, HPs & EVs. The suburban area has the most serious violations, especially the heavy grid, under both seasons and all LCT (loading) conditions, which can reach up to 800% T/F over-loading. It is noteworthy that the Winter season always provokes greater violations than Summer, reaching up to double value in the heavy suburban grid at 100% combined LCT penetrations. Furthermore, the HP loading condition is also at most grids heavier than the EV loading condition. For example, the EV loading condition does not overload the T/Fs of the Urban area, while HP loading can reach up to 3–4 times higher in the suburban areas.

Moreover, a T/F loading decrease is observed at the light suburban grid for EV loading from 50% to 80%, which means that the increased PV generation can cover more efficiently the increased EV charging demand. This phenomenon is not seen for HP loading. The behavior of the slopes is also very important. Saturation can be seen in the light rural grid for all cases from 80% until 100% penetration. We can conclude that for most of the cases at the other grids, the increase presents a rather linear behavior, apart from the exponential increase at the heavy suburban grid for combined 100% penetrations of LCTs.

Fig. 7 depicts the total over-loading duration and DMP (violation area) for the 6 grids, under 100% penetration of combined PVs-EVs-HPs during Winter. While both problems are crucial in the heavy

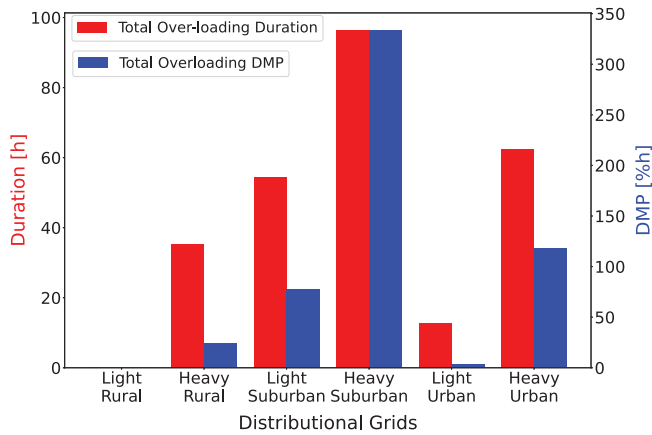


Fig. 7. Total Overloading Duration and DMP under combined PVs-EVs-HPs 100% penetration during Winter.

Suburban area (reaching approximately 95 h total violation duration and 330 [%h] DMP), comparing the other grids' respective results with this area, duration is of greater importance for the rest of the grids. However, apart from the light rural area, which is not violated, the transition from light-loaded to heavy-loaded grids increases the DMP more than the total violation duration. Especially for the urban case, the duration increases 4.4 times, while the respective number for the DMP is approximately 38.5.

Finally, Fig. 8 summarizes the comparison between EV & HP loading in the most vulnerable distribution grids. The magnitude and the duration of each T/F over-loading incident are depicted (during both seasons) at 50, 80 & 100% penetrations. The higher grid impact of the Winter over the Summer season and of the HP over the EV loading can also be seen here. All Winter overloading incidents for both loading conditions are shifted to the upper and/or right direction in the plots (higher magnitude and/or higher duration), compared with the respective summer incidents, and are significantly more at all penetrations. Moreover, the heavy urban grid until 80% penetration and the light suburban grid are not affected by EV loading. In agreement with Fig. 7, in the heavy grids, higher penetrations provoke more overloading incidents and prolonged durations rather than higher violation magnitudes. However, in the case of the light urban grid, the violation magnitudes are barely increased during higher penetrations, while there is a notable increase in violation times and durations, which can reach up to 300'. Hence, the significance of the duration in the lighter grids is also seen here.

Last but not least, it is important to mention that when overloading is caused by EV loading, it is typically seen at the lower-right place in the plots (higher durations-lower magnitudes). On the contrary, violations by HP loading are typically seen at the left place in the plots and are characterized by higher magnitudes. For example, no HP violations surpass 300', while EV violations in heavy grids can reach up to 500'. This is an outcome of the use of real models of the LCTs in our work. EV charging endures for several hours. However, while rated EV charging power is much higher than HP power (at least 11 kW as seen in Fig. 2), people use their HPs more frequently than they charge their EVs. Hence, the fewer but long-lasting over-loading times by EV loading are justified. The more frequent HP operation causes notably more overloading incidents. The simultaneous ON-OFF operation of the HPs in the distribution grids results in remarkably higher over-loading magnitudes. However, the violations endure less because the HPs switch to the OFF stage as soon as the desired building temperatures are reached (typically in 30'), which is faster than the typical EV charging duration.

5.3. Lines overloading

The maximum grid line loading (extracted from all the lines) is depicted in Fig. 9 at the 6 grids for 50, 80 & 100% penetrations of combined PVs, EVs & HPs. Moreover, the total number of overloaded lines, for 100% penetration at every time instant, can be seen as well. The selected results refer to the Winter season since its higher grid impact has already been seen in the previous subsection.

The heaviest grid impact on suburban grids is again seen in Fig. 9. The light rural grid is again the only one that does not suffer from overloading, while overloading happens at the heavy rural grid from 80% and can reach up to 60 simultaneously overloaded lines. However, the suburban grids are both overloaded from 50% combined LCTs penetration, with heavy suburban grid having lines exceeding 700% overloading and reaching approximately 400 overloaded lines (approximately the maximum 30.2% of the total lines). Furthermore, the overloading time incidents are vastly more in the suburban area. It is also very important to note the significance of the simultaneous violated locations at the grids. Similar overloading, in terms of violation times and magnitude, is seen at the light and heavy urban grids for all 3 penetrations. However, the number of simultaneously overloaded lines is double at the heavy grid (maximum 25 lines for the light urban grid, whereas over 60 lines for the heavy one).

A comparison of 100% EV and HP loading at the 3 heaviest grids is presented in Fig. 10. The overloading DMP of all the grid lines is depicted in Fig. 10(a), while the total overloading time is depicted in Fig. 10(b). Most of our previous insights are also strengthened here. Regarding EV and HP loading conditions comparison, HPs also produce worse results regarding the lines loading. For example, heavy urban and light suburban grids are minimally or not affected by EV loading, while HP loading overloads the same grids for 35 h and 28 h, respectively. Moreover, the heavy suburban grid's DMP can reach up to 12%h, which is considerably higher than the respective one by EV loading. The DMP median is close to 4.9%h, and the maximum is more than 6x the related maximum by EV loading, even though some outliers reaching up to 5.5%h can be seen. However, at the same grid, the overloading time of EV loading, in contrast with the respective DMP, can reach up to 48 h, only 17.2% less than the overloading time by HP loading. This comes in agreement with Fig. 8, which suggests that EV loading inflicts long-lasting overloading durations with however low magnitude. Finally, compared with the heavy suburban grid, the total violation duration of the other two grids are more comparable than the respective DMPs, reaching a maximum of only 2 times lower. This also strengthens the insight that duration is more significant than violation area in the lighter grids.

5.4. Nodes voltage deviation: Under-/Over-voltage (UV & OV)

Overvoltage (OV) issues are more likely to appear during the Summer season due to increased PV generation, while undervoltage (UV) issues are more severe during the Winter season when HP and EV consumption is higher. Therefore, the minimum node voltage (of all the nodes) at every time instant for 50, 80 & 100% penetrations of combined LCTs at the 6 grids during the Winter season is depicted in Fig. 11. In addition, the maximum node voltage at 100% penetration during Summer is integrated. No overvoltage is seen at any of the 6 investigated Dutch distribution grids since the maximum node voltage always stays below 1.1 p.u. Furthermore, no undervoltage is seen in the investigated rural and urban areas since the minimum node voltage always stays above 0.9 p.u. However, suburban grids are severely affected by undervoltage. The light suburban grid sees a voltage drop under 0.9 p.u. even from 50% penetration (once), while also once voltage drops under 0.85 p.u. at 100% penetration. Multiple undervoltage incidents are observed in the heavy suburban grid at all 3 penetrations. Reaching up to 0.65 p.u. and 0.42 p.u. at 80% and 100%

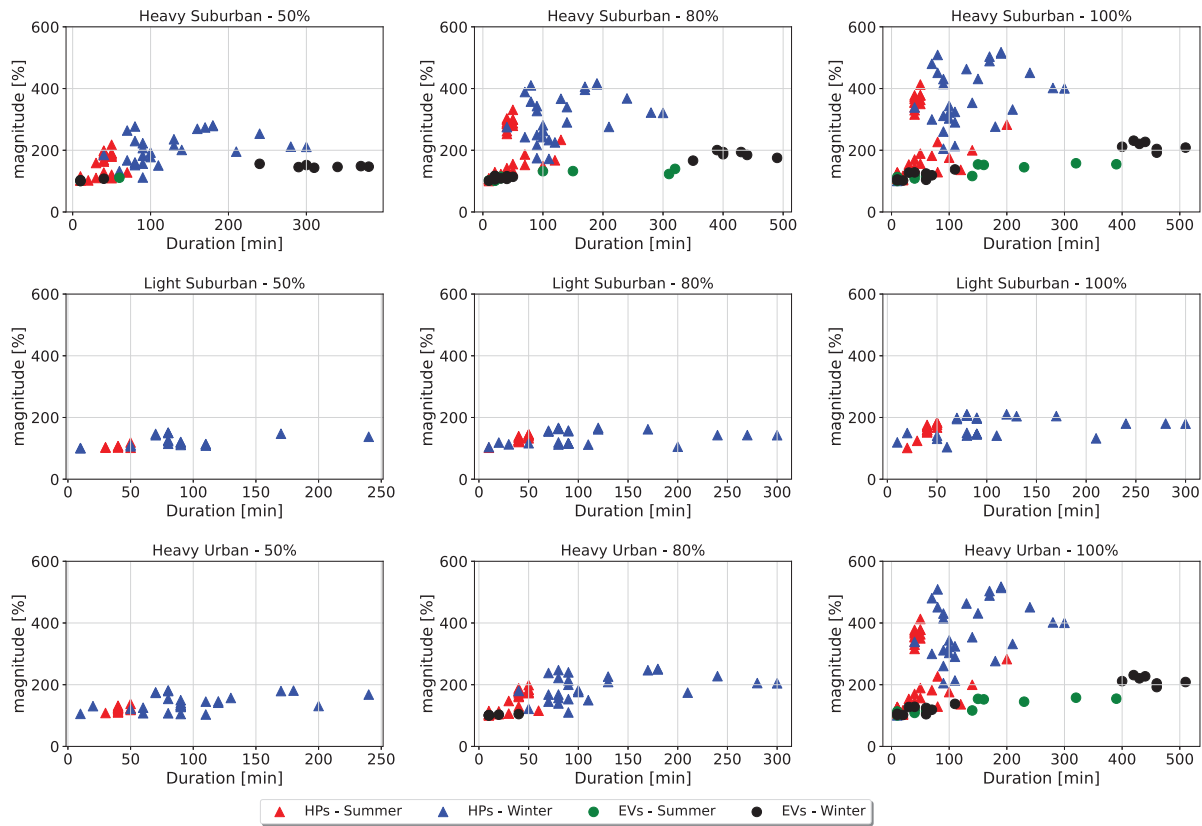


Fig. 8. Duration and Magnitude of each overloading incident at the 3 most vulnerable distributional areas under HP & EV load conditions and 50, 80, 100% penetrations.

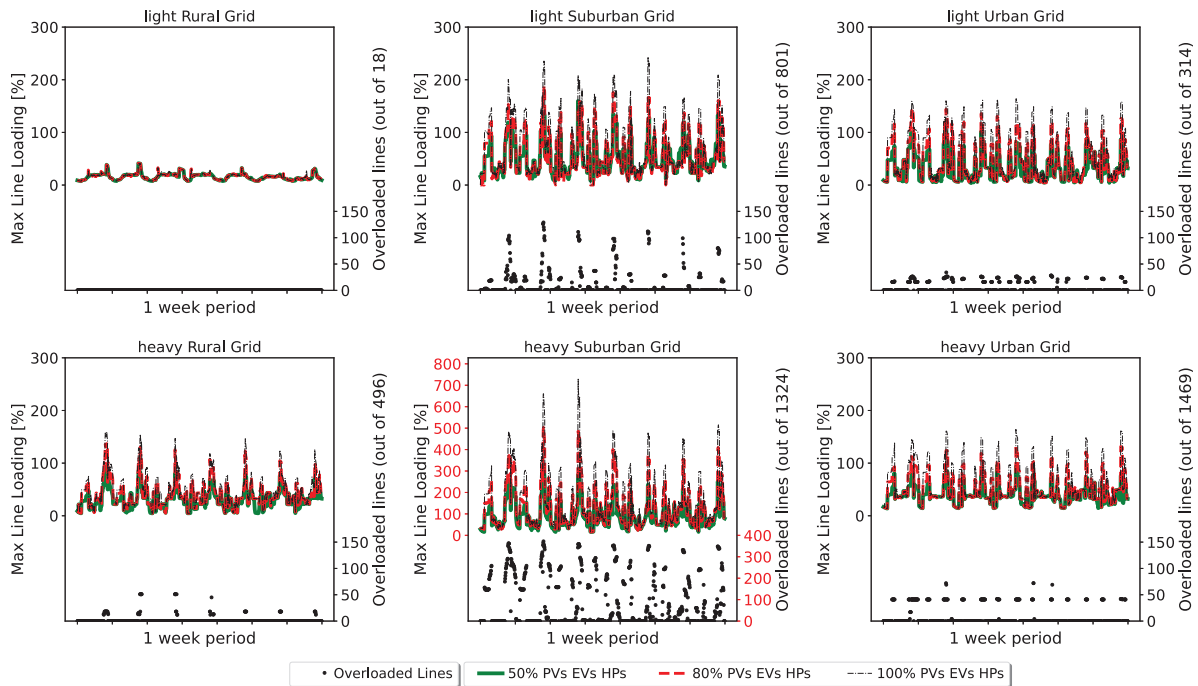


Fig. 9. Max Line Loading (of all grid lines) under 50, 80 & 100% and Number of Over-loaded Lines under 100% penetrations of combined PVs, EVs, HPs during Winter season.

penetrations, respectively, combined LCTs penetrations vastly distort the node voltage profile at the heavy suburban grid.

The comparison of HP and EV loading regarding UV is summarized in Fig. 12, which depicts the maximum UV magnitude and number of violated nodes at 50% and 100% penetrations for the heavy suburban grid. The greater grid impact regarding voltage deviation of the HP

loading can also be seen here. At both 50% & 100% loading, HP causes more times UV issues with higher magnitude. For example, 50% HP loading causes UV 21 times with a max drop of 0.058 below 0.9 p.u. and 590 violated nodes. The related values of 50% EV loading are 10 times, 0.018 p.u. max drop and 53 nodes. Additionally, the long-term low-magnitude grid impact characteristic of EV loading compared to

Table 6
Comparison of grid impact for bottom-up & top-down approaches during 100% penetration of PVs, EVs & HPs.

	Transformer (Over-)loading				Lines maximum (Over-)loading				Nodes (Under-)voltage			
	bottom-up		top-down		bottom-up		top-down		bottom-up		top-down	
	max%	Time%	max%	Time%	max%	Time%	max%	Time%	min p.u	Time%	min p.u	Time%
Winter-rural	203.38	21	132.08	10.7	159.54	7	120.96	1.6	0.911	0	0.941	0
Winter-urban	331.35	37.2	191.79	53.9	164.03	18.4	102.36	0.1	0.899	0.3	0.936	0
Winter-suburban	781.63	57.4	395.19	83.3	728.54	51.3	306.72	69.2	0.42	44.6	0.763	48.6
Summer-rural	147.75	3.6	75.41	0	132.9	1.4	79.64	0	0.936	0	0.96	0
Summer-urban	258.25	13.4	155.56	6.3	124.87	4.66	88.62	0	0.923	0	0.962	0
Summer-suburban	521.66	31.3	252.51	31.7	413.72	22.7	179.98	19.8	0.675	14.6	0.859	4.8

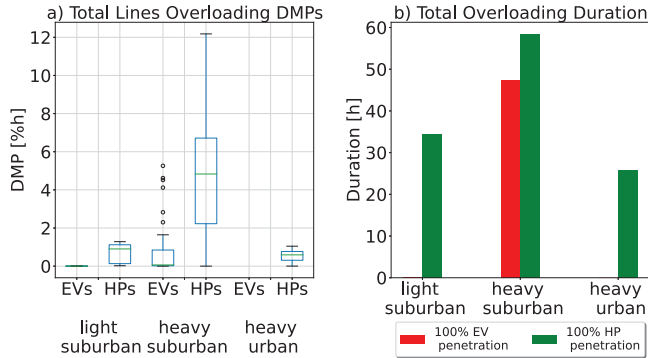


Fig. 10. Total overloading DMP (a) & Duration (b) at the 3 most vulnerable areas under 100% of EV & HP loading.

HP loading can be seen at 100% loading, where multiple UV times can be seen with duration over 200' up to 400', but with 50% fewer max simultaneously violated nodes and 65% lower maximum voltage drop.

5.5. Comparison of grid impact issues

In the previous subsections, useful insights have been derived by comparing directly different distributional areas, seasons, and EV-HP loading for every considered grid impact issue. This section is devoted to the comparison of these grid impact issues. In Fig. 13, the magnitude & duration of the four important investigated grid impact issues are compared regarding the different distributional areas (DA comparison) and LCT integration (LCT comparison) and depending on the utilized grid impact metrics. The definitions “High (H)”, “Medium (M)”, “Low (L)” and “Zero (Z)” are defined as follows:

- Z: No impact.
- L: Violation occurs only in heavy grids and < 50% magnitude - 3% duration.
- M: Violation occurs in heavy and light grids and < 100% violation - 25% duration.
- H: Violation occurs in heavy and light grids and > 100% violation - 25% duration.

Observing the 2 heatmaps, it is concluded that T/F O/L is the most crucial grid impact issue for the 6 assessed grid case studies in terms of both magnitude and duration, followed by lines overloading and consequently by node UV in both DA and LCT comparisons. No node OV has been observed in this work.

5.6. Bottom-up & Top-down approaches comparison

The analysis in Sections 5.1–5.5 is conducted with the use of physical models from Sections 3.2–3.4 since this work constitutes a bottom-up approach. However, simulations under the same case studies have been performed with the use of aggregated data from Section 3.1. for all considered LCTs (top-down approach). The contribution of this

subsection is the comparison and cross-validation of the two different approaches, mostly used in grid impact studies, which are summarized in Table 6. In Table 6, the total violation magnitude and time in % are presented for the transformer loading, lines maximum loading, and node minimum voltage at the 3 different heavily-loaded grids during Winter and Summer under 100% penetration of PVs, EVs & HPs for the two approaches.

It can be seen that when a bottom-up approach is used, the magnitude of all grid impact issues is greater for all distributional areas and seasons. Additionally, the highest differences between the two approaches can be seen in the suburban grid. For example, suburban grid lines are by approximately half overloaded in the top-down approach (57.9% and 56.5% reduction for Winter and Summer seasons, respectively). Moreover, a related 49.44% and 51.59% reduction of the T/F loading is also seen in the same grid for the two seasons. Considering that the suburban area is already found to be the most vulnerable one due to a high number of nodes and loads, it can be concluded that the vulnerability of an area enhances the difference between the two approaches. Similar observations can also be made for the nodes’ undervoltage issue. On the contrary, different seasons do not seem to have a consistent effect on the comparison of the approaches since contradictory results can be seen. A higher reduction is seen for the rural area during Summer, while the opposite is seen for the urban area.

However, an interesting insight from this comparison is that the total violation duration does not always follow the same trend as the maximum magnitude. In 3 different scenarios (Urban area—Winter, Suburban—Summer & Suburban—Winter), the total violation duration of grid impact issues is found to be higher in the top-down approach. These observations are marked in red color in Table 6. Especially for the suburban area during Winter, this can be seen for all 3 grid impact issues. More specifically, the total duration of the transformer overloading rises by 45.1%, while the overloading duration of the lines rises by 34.9%, which corresponds to approximately 76 h and 58.5, respectively. Moreover, most of these observations belong to the transformer overloading issue.

The above contradiction regarding the violations’ magnitude and duration can be justified if we consider the nature of the two approaches. Regarding the top-down approaches, the use of nationally aggregated data, extrapolated to the appropriate level, contains characteristics of different areas, which enhance sparsity and tend to average results over time. On the contrary, the use of physical models can better capture the effect of simultaneous components’ operation and therefore produce higher peaks, spikes, and violations’ magnitude. This can also be seen in Fig. 14, which compares the top-down and bottom-up results for the transformer loading and nodes’ minimum voltage at the heavy urban grid at 100% penetration of LCTs during Winter. In both cases, the bottom-up results are characterized by more spikes and higher slopes than the more dispersed top-down results, which occupy more area by width. Hence, this can lead to the disappearance of violation if a grid is lightly loaded. However, if a grid is heavily loaded enough, this can lead to higher violation durations. Furthermore, these cases belong mostly to the transformer loading because all of the investigated grids comprise an LV transformer, which handles all the power flow.

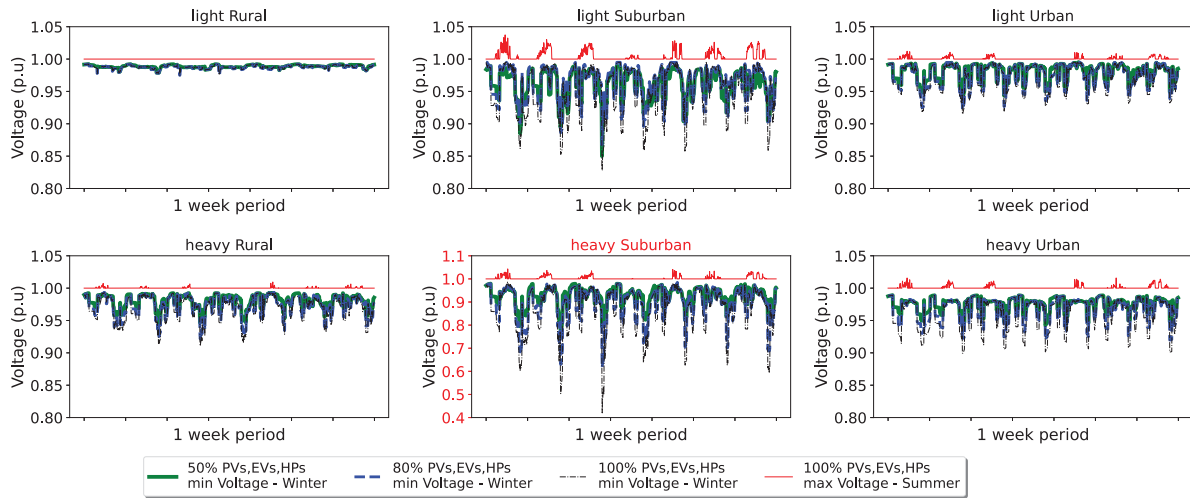


Fig. 11. Min Node Voltage during Winter under 50, 80 & 100% and Max Node Voltage during Summer under 100% penetrations of combined PVs, EVs, HPs.

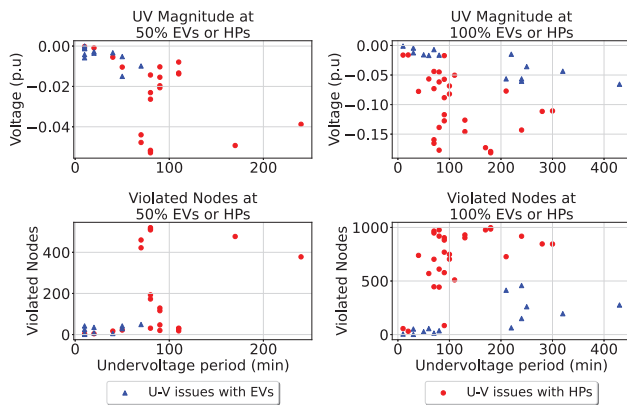


Fig. 12. Max Undervoltage & violated nodes at heavy Suburban grid under 50 & 100% of EV and HP loading.

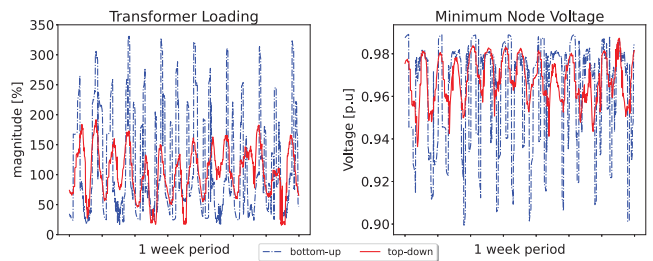


Fig. 14. T/F Loading & Nodes Min Voltage for top-down and bottom-up approaches (heavy urban grid, 100% LCTs penetration, Winter).

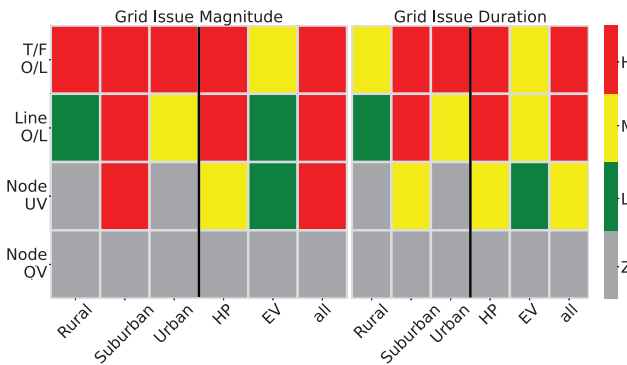


Fig. 13. Grid Issues Evaluation (Magnitude & Duration).

Therefore, due to the aggregated power flow through the transformer, this can happen easier for the particular grid impact issue.

However, observing Table 6, it must be noted that despite the differences between the two approaches, the main insights from the bottom-up analysis remain the same. The suburban grid remains the most vulnerable distributional area, the transformer overloading the most critical grid impact issue, and also the Winter season provokes more significant violations than the Summer season. Therefore, the two approaches are also well cross-validated.

6. Discussion of results

6.1. Summary of findings

The most important work's findings are summarized below, divided into the following categories:

- I: findings that agree with the existing literature.
- II: findings that contradict the existing literature. Existing contradictions in the literature are also integrated here.
- III: new insights.

Regarding Category I, firstly, Winter is considered overall a heavier season than Summer, due to the higher heating and transportation load, in terms of all investigated grid impact issues, which comes in agreement with many works, such as [4] & [30]. On the one hand, this is justified by the higher EV consumption during Winter due to cabin heating and by the higher HP consumption due to lower COPs. On the other hand, it is justified by the low PV generation during Winter. Secondly, mitigation of grid impact issues during increasing combined EV-PV penetrations, such as in [8], have also been observed here in the light suburban grid from 50% to 80% penetration (see Fig. 6). EV charging, especially at semi-public and public chargers, has higher chances of time overlap with PV generation, and therefore, mitigation of issues at higher penetrations is expected in some cases. Finally, such as in [28], overvoltage is less likely to appear also for the grids of this work in high PV penetrations due to simultaneously high EV & HP loading (Fig. 11).

The contradictions of this work are integrated into Category II, which at most times, refers to already contradicted findings in the literature. The impacts of HPs and EVs have already been compared in the literature. Increasing EV penetrations were found to cause higher T/F

overloading in [33,37]. EVs were also characterized by higher power peaks in [32]. On the contrary, higher voltage deviations were caused by HPs in [9], while higher T/F and lines overloading appeared in [24]. In this work's grid case studies, HPs are found to be a heavier LCT to be integrated into the grid in terms of total violation magnitude, duration, DMP, and number of incidents. This is justified, firstly, by the fact that we completely respected the thermal comfort of the households. Charging sessions are less frequent than the operation of the HPs to keep the temperature of the buildings at the desired level. Secondly, as already explained, the use of components' models, which directly model their physical operation, produces more dense and simultaneous consumption. On the contrary, top-down works, such as [32] & [33], used extrapolated aggregated data, which are usually more dispersed. This difference heavily affects the consumption results of the HPs, which continuously maintain the desired buildings' temperature.

Suburban and rural grids were found to be more vulnerable regarding voltage deviations and T/F loading in [7]. Line overloading also appeared from low EV penetrations in suburban grids in [16], while rural grids were more violated than urban ones in [6] & [3]. In this work, the Dutch suburban areas were vastly violated in all cases compared to the other two areas, while grid impact issues in Dutch rural areas appeared less frequently. The main reason for this contradiction comes directly from the difference in the grid loads. The utilized rural, suburban & urban grids in this work are real LV grids from the Netherlands, where city suburbs are overpopulated (see Table 1). On the contrary, the rural grids are typically characterized by a lower number of loads. As can be seen in Table 4, especially the light rural grid comprises only 3 commercial buildings. This directly decreases the chances and magnitude of violations in rural areas.

Another popular debate in the literature is about the most hazardous grid impact issue. In the grids of this work, overvoltage was not seen, while undervoltage was seen less frequently and mostly in the suburban area. On the contrary, overloading, especially of T/Fs, is the most crucial issue under all conditions regarding both duration and magnitude. Authors in [14] & [24] agreed with the superiority of T/F overloading. On the contrary, cable overloading appeared from lower penetrations in [3]. However, voltage issues were more severe than line overloading in [14] & [15]. The absence of overvoltage is because consumption remains high also in Summer since we respected the thermal and transportation comfort of the population (e.g. reversible HPs). Moreover, it is justified by the rather moderate Dutch Summers with respect to Dutch Winters. The significance of the T/F overloading was expected since all 6 used grids are fed by an MV/LV T/F, which is burdened with all grid power exchange.

The explained points of category II are already well-known contradictions in the literature. In this work, efforts have been made to address them, considering various effects that can considerably impact their results. Moreover, real grids have been used for this purpose. However, according to the authors' point of view, the insights of these comparisons are highly dependent on the characteristics of the different case studies in the various works, such as grid locations, grid characteristics, consumers' behavior, etc. Therefore, they can be very grid-specific and can result in contradictions. For example, especially, voltage deviations are highly subject to the parameters of the components of the different grid topologies, e.g. of the distribution lines. In this work, a higher level of overloading than of undervoltage incidents is found in many cases, e.g. at heavy rural, light urban, and heavy urban grids at 80% and 100% LCT penetrations. This is highly dependent on the specification of the Dutch distribution grid case studies, the adequacy of reactive power in the networks, the power factor of the loads, etc. Hence, the respective findings should only be carefully considered and not be effortlessly over-generalized for every investigated grid case study.

Finally, regarding category III, this work's new findings can be summarized as follows. Observing Fig. 6, saturation is seen for the transformer (over)loading under increasing penetrations of LCTs in the

light rural grid (least population). In contrast, exponential behavior is seen in the heavy suburban grid (highest population), while linear behavior is observed in the rest of the grids. Hence, the nature of grid nodes and loads directly affects the behavior of the slope of the T/F maximum loading curve.

In Fig. 6, we can also see that while increasing EV-PV penetrations can mitigate grid impact issues such as T/F overloading, this is not seen in HP-PV penetrations. The long-lasting (often several hours) and high-powered (> 11 kW) EV charging sessions appear to favor more mitigation than the HP ON time period, which is typically shorter-term and with less power (max of 2–3 kW). Moreover, the HPs are less easily temporarily combined with PVs, because the PV generation is at its highest when the buildings are not occupied.

In several figures, such as Figs. 7, 8 and 10, it can be seen that violation duration plays a more important role in the lighter grids than magnitude (in total). However, upon transition to the heavier grids, the magnitude and the DMP of the violations increase vastly compared with the respective duration. The lower magnitude and DMP of the violations in the lighter grids are justified by the lower number of integrated loads and LCTs. However, while the number of loads increases greatly in the heavier grids, their time of operation does not change that much. For example, it has been assumed that in both grids, people leave and return to their buildings or charge their EVs at home or at work during similar time periods. Therefore, this adds up to the loading of the LCTs, greatly increasing the total magnitude, but the impact on the total violation duration is considerably less.

Furthermore, in Figs. 8, 10 and 12, specific violations (T/F overloading and node undervoltage, respectively) by EVs are more likely to have smaller magnitude and longer duration, in contrast with the HPs. This is also justified by the long-lasting EV charging sessions compared with the ON-OFF operation of the HPs. However, the number of violation incidents under HP integration increases vastly, and the total violation duration exceeds the one by EV integration.

Finally, according to the authors' knowledge, a comparison of bottom-up and top-down approaches for grid impact studies has not yet been conducted in the existing literature. Bottom-up approaches have been found to produce violations of higher magnitude due to the simultaneous operation of the components. However, top-down approaches can produce violations with longer-term duration because they tend to average the results over time.

6.2. Recommendations

In light of this work's findings, the authors take the initiative to provide the following recommendations. While a yearly grid impact assessment is always highly recommended in grid impact studies, the investigation of worst-case scenarios during Winter should always be prioritized. Additionally, it is recommended that the DSOs consider carefully the already existing loading condition of the inspected grids, which can play a vital role in the increase of the grid impact by the LCTs. For example, Dutch suburban grids will probably require a higher level of grid investments and/or a higher level of power control for impact minimization, due to the fact that they are usually over-populated.

Moreover, the mitigation of grid impact issues by the PVs-EVs combination shows that there is more "room" for power control between these 2 LCTs with the aim of lower grid investments. On the contrary, an efficient PVs-HPs combination is more difficult to be achieved, and hence, the use of energy storage or of a higher energy storage size is more important in this case.

While the authors of this work realize the importance of the investigated grid selection in their results, they recommend that high focus is placed on the future HPs integration. The higher insulation and the improvement of the energy label of the future buildings are highly recommended for the minimization of the grid impact by the future electric heating. Similarly, T/F overloading is highly expected for LV

grids that are fed only by an MV/LV T/F, because the T/F handles all the power flow. However, due to the observed contradictions depending on the grid and case study selection, it is advised that all impact issues are investigated under individual or combined LCTs integration. In that way, insights can be drawn concerning the connection of LCTs with impact issues for the inspected case, and hence, an appropriate issue weight factor is given for the needed grid investments.

Regarding the fact that violation magnitude becomes more important in heavier-loaded distribution grids, a high focus should be given to the selection of the appropriate simultaneity factor concerning the investigated grid. The simultaneity factor is grid-specific and the already existing grid loading condition should be considered, before its estimation in grid impact studies.

Furthermore, as already explained, both top-down and bottom-up approaches have reverse advantages and disadvantages. Despite their difference, the main insights of this work remained similar with the use of both approaches. Therefore, it is advisable that both approaches are followed for every grid impact analysis so that the results are cross-validated.

Overall, this work shows that grid impact issues are expected even from 50% of combined LCTs penetrations. The authors believe that grid-specific power control of LCTs with or without energy storage, operated by the future DSOs, will be indispensable for future LCTs integration so that the needed level of future grid investments is decreased as much as possible.

7. Conclusion and future work

In this work, several grid impact issues are addressed in real LV Dutch distribution grids, caused by increasing LCT penetrations, such as PVs, EVs & HPs. Despite the dependence of the results on the assumptions and specifications of the case studies, the findings of this work can provide grid operators, especially in the Netherlands, with valuable insights about the grid impact from future LCT integration and the various factors that affect it. Comparisons are made between different seasons, distributional areas, LCTs, and LCT penetrations showing the greater hazards for the Winter season, the Dutch suburban grids & HP integration. Winter is characterized by higher consumption in the heating and transportation sectors, while the Dutch suburban grids are vulnerable due to the higher number of grid loads. The more frequent use of HPs for heating/cooling provokes a higher grid impact overall, but the longer EV charging periods provoke more long-lasting violations. Detailed LCT physical models have been used in the analysis in order to follow a bottom-up approach, considering the physical layer of the component operation. The results have also been compared with results by aggregated data from databases, showing that bottom-up approaches present more pessimistic results than top-down approaches, however, the main insights remain similar. However, higher violation durations can be seen when a top-down approach is used, due to the higher sparsity of the results.

This work has inserted a level of uncertainty during the development of the used physical models. Examples of considered uncertainties are the randomization of the orientation of the PV modules, buildings occupation, distribution of LCTs in the distribution grids as well as the use of MCS for the generation of the EV charging profiles. However, many more sources of uncertainties exist in grid impact studies, such as different properties of buildings and technologies, that should also be encapsulated. This is considered the main limitation of this work. Moreover, this work comprises only slow AC EV charging, whereas DC fast charging will also be a main feature of the future of electrified transportation. Additionally, another limitation of this work is that all LCTs and loads are considered balanced. However, the electrification of generation and demand also conceals great hazards regarding the level of future grid imbalance, which can further enhance the investigated issues. Finally, the identified grid impact of this work can be highly decreased with the use of the flexibility of the loads (EVs and HPs) and of energy storage. All of the above are recommended as future work of this investigation.

CRedit authorship contribution statement

Nikolaos Damianakis: Writing – review & editing, Writing – original draft, Validation, Software, Methodology, Investigation, Data curation, Conceptualization. **Gautham Ram Chandra Mouli:** Writing – review & editing, Supervision, Resources, Project administration, Funding acquisition. **Pavol Bauer:** Writing – review & editing, Supervision, Project administration, Funding acquisition. **Yunhe Yu:** Writing – review & editing, Software, Methodology, Investigation.

Declaration of competing interest

The authors declare the following financial interests/personal relationships which may be considered as potential competing interests: Nikolaos Damianakis reports financial support was provided by Dutch Research Council.

Data availability

Data will be made available on request

Acknowledgments

This study is funded by the Dutch Research Council (NWO) as part of the ongoing research project NEON with project number 17628 of the research program Crossover. Moreover, I would like to thank Enexis Groep for the acquisition of the 6 distribution grids, and personally, Arjan Wargers, Bregje Vos & Arjan van Voorden for their valuable advice.

References

- [1] Rüdüsili M, Teske S, Elber U. Impacts of an increased substitution of fossil energy carriers with electricity-based technologies on the swiss electricity system. 2019, <http://dx.doi.org/10.20944/preprints201905.0179.v1>.
- [2] Asare-Bediako B, Kling W, Ribeiro P. Future residential load profiles: Scenario-based analysis of high penetration of heavy loads and distributed generation. *Energy Build* 2014;75:228–38, [Online]. Available: <https://www.sciencedirect.com/science/article/pii/S037877881400139X>.
- [3] Protopapadaki C, Saelens D. Heat pump and PV impact on residential low-voltage distribution grids as a function of building and district properties. *Appl Energy* 2017;192:268–81, [Online]. Available: <https://www.sciencedirect.com/science/article/pii/S0306261916317329>.
- [4] Oliyide RO, Cipcigan LM. The impacts of electric vehicles and heat pumps load profiles on low voltage distribution networks in Great Britain by 2050. *Int Multidiscip Res J* 2021;11:30–45.
- [5] Eurostat. Greenhouse gas emissions by source sector, EU, 2020. 2022, <https://www.weforum.org/agenda/2022/09/eu-greenhouse-gas-emissions-transport/>. [Accessed: 28 May 2023].
- [6] Gupta R, Pena-Bello A, Streicher KN, Roduner C, Farhat Y, Thöni D, et al. Spatial analysis of distribution grid capacity and costs to enable massive deployment of PV, electric mobility and electric heating. *Appl Energy* 2021;287:116504, [Online]. Available: <https://www.sciencedirect.com/science/article/pii/S0306261921000623>.
- [7] Thormann B, Kienberger T. Evaluation of grid capacities for integrating future E-mobility and heat pumps into low-voltage grids. *Energies* 2020;13:5083.
- [8] Brinkel N, Gerritsma M, AlSkaif T, Lampropoulos I, van Voorden A, Fidder H, et al. Impact of rapid PV fluctuations on power quality in the low-voltage grid and mitigation strategies using electric vehicles. *Int J Electr Power Energy Syst* 2020;118:105741, [Online]. Available: <https://www.sciencedirect.com/science/article/pii/S0142061519319994>.
- [9] Navarro-Espinosa A, Ochoa LF. Probabilistic impact assessment of low carbon technologies in LV distribution systems. *IEEE Trans Power Syst* 2016;31(3):2192–203.
- [10] Antić T, Capuder T, Bolfek M. A comprehensive analysis of the voltage unbalance factor in PV and EV rich non-synthetic low voltage distribution networks. *Energies* 2020;14.
- [11] Kong W, Ma K, Li F. Probabilistic impact assessment of phase power imbalance in the LV networks with increasing penetrations of low carbon technologies. *Electr Power Syst Res* 2022;202:107607, [Online]. Available: <https://www.sciencedirect.com/science/article/pii/S0378779621005885>.
- [12] Uriarte FM, Hebner RE. Residential smart grids: Before and after the appearance of PVs and EVs. In: 2014 IEEE international conference on smart grid communications. 2014, p. 578–83.

- [13] Mueller S, Moeller F, Klatt M, Meyer J, Schegner P. Impact of large-scale integration of E-mobility and photovoltaics on power quality in low voltage networks. In: International ETG congress 2017. 2017, p. 1–6.
- [14] van der Burgt J, Vera SP, Wille-Haussmann B, Andersen AN, Tambjerg LH. Grid impact of charging electric vehicles; Study cases in Denmark, Germany and The Netherlands. In: 2015 IEEE Eindhoven powertech. 2015, p. 1–6.
- [15] Gabdullin Y, Azzopardi B. Impacts of high penetration of photovoltaic integration in Malta. In: 2018 IEEE 7th world conference on photovoltaic energy conversion. 2018, p. 1398–401.
- [16] Kotsonias A, Hadjidemetriou L, Kyriakides E, Ioannou Y. Operation of a low voltage distribution grid in cyprus and the impact of photovoltaics and electric vehicles. In: 2019 IEEE PES innovative smart grid technologies Europe. 2019, p. 1–5.
- [17] Ramaswamy PC, Chardonnet C, Rapoport S, Czajkowski C, Sanchez RR, Gomez Arriola I, et al. Impact of electric vehicles on distribution network operation: Real world case studies. In: CIRED workshop 2016. 2016, p. 1–4.
- [18] Niitsoo J, Taklaja P, Palu I, Klüss J. Power quality issues concerning photovoltaic generation and electrical vehicle loads in distribution grids. *Smart Grid and Renewable Energy* 2015;06:164–77.
- [19] Ceylan O, Paudyal S, Dahal S, Karki NR. Assessment of harmonic distortion on distribution feeders with electric vehicles and residential PVs. In: 2017 7th international conference on power systems. 2017, p. 621–6.
- [20] Liang J, Qiu YL, Xing B. Impacts of the co-adoption of electric vehicles and solar panel systems: Empirical evidence of changes in electricity demand and consumer behaviors from household smart meter data. *Energy Econ* 2022;112:106170, [Online]. Available: <https://www.sciencedirect.com/science/article/pii/S0140988322003231>.
- [21] Fachrizal R, Ramadhani UH, Munkhammar J, Widén J. Combined PV–EV hosting capacity assessment for a residential LV distribution grid with smart EV charging and PV curtailment. *Sustain Energy Grids Netw* 2021;26:100445, [Online]. Available: <https://www.sciencedirect.com/science/article/pii/S2352467721000163>.
- [22] Haakana J, Haapaniemi J, Lassila J, Partanen J, Niska H, Rautiainen A. Effects of electric vehicles and heat pumps on long-term electricity consumption scenarios for rural areas in the nordic environment. In: 2018 15th international conference on the european energy market. 2018, p. 1–5.
- [23] Li Y, Crossley PA. Monte Carlo study on impact of electric vehicles and heat pumps on LV feeder voltages. In: 12th IET international conference on developments in power system protection. 2014, p. 1–6.
- [24] Hulsman L, Schloser T, Koch M, Ohl U. Electric vehicle and heat pump hosting capacity assessment for a german 25,000-noded distribution network. In: 21 wind & solar integration workshop. 2022-10-12, [Online]. Available: <https://windintegrationworkshop.org/downloads/>.
- [25] Kelly N, Hand J, Samuel A. Modelling the impact of integrated electric vehicle charging and domestic heating strategies on future energy demands. 2014.
- [26] Yang F, Yan F, Liu H, Shan W, Xu X, Dong X. Coordination of heat pumps and electric vehicles in residential distribution network voltage control. 2021, p. 1–5. <http://dx.doi.org/10.1145/3469213.3471359>.
- [27] Meunier S, Protopapadaki C, Baetens R, Saelens D. Impact of residential low-carbon technologies on low-voltage grid reinforcements. *Appl Energy* 2021;297:117057, [Online]. Available: <https://www.sciencedirect.com/science/article/pii/S0306261921005146>.
- [28] Coumans DJS, Grond MOW, Coster EJ. Impacts of future residential electricity demand and storage systems on 'classic' LV-network design. In: 2015 IEEE Eindhoven powertech. 2015, p. 1–6.
- [29] Van Someren C, Visser M, Sloopweg H. Impacts of electric heat pumps and rooftop solar panels on residential electricity distribution grids. In: 2021 IEEE PES innovative smart grid technologies Europe. 2021, p. 01–6.
- [30] Protopapadaki C, Saelens D. Sensitivity of low-voltage grid impact indicators to weather conditions in residential district energy modeling. 2018.
- [31] Fischer D, Surmann A, Lindberg KB. Impact of emerging technologies on the electricity load profile of residential areas. *Energy Build* 2020;208:109614, [Online]. Available: <https://www.sciencedirect.com/science/article/pii/S0378778819309594>.
- [32] Fischer D, Scherer J, Flunk A, Kreifels N, Byskov-Lindberg K, Wille-Haussmann B. Impact of HP, CHP, PV and EVs on households' electric load profiles. In: 2015 IEEE Eindhoven powertech. 2015, p. 1–6.
- [33] Viganò G, Clerici D, Michelangeli C, Moneta D, Bosisio A, Morotti A, et al. Energy transition through PVs, EVs, and HPs: A case study to assess the impact on the Brescia distribution network. In: 2021 AEIT international annual conference. 2021, p. 1–6.
- [34] van Zoest P, Veldman E, Lukszo Z, Herder P. Analysis of future electricity demand and supply in the low voltage distribution grid. In: Proceedings of the 11th IEEE international conference on networking, sensing and control. 2014, p. 619–24.
- [35] Bhattacharyya S, Wijnand M, Slangen T. Estimating the future impact of residential EV loads on low voltage distribution networks. In: CIRED porto workshop 2022: e-mobility and power distribution systems, vol. 2022. 2022, p. 128–32.
- [36] Al Essa MJM, Cipcigan LM. Integration of renewable resources into low voltage grids stochastically. In: 2016 IEEE international energy conference. 2016, p. 1–5.
- [37] Rafi A, Lee T, Wu W. Impact of low-carbon technologies on the power distribution network. *IOP Conf Ser: Earth Environ Sci* 2019;329(1):012055.
- [38] Galvin R, Quinn S, Hunt S, White P, Murray D, Tierney V, et al. System wide power flow analysis of the irish distribution network to assess the impact of projected low carbon technology loads and generation including significant increase of electric vehicles connected to the grid. In: CIRED Porto workshop 2022: e-mobility and power distribution systems, vol. 2022. 2022, p. 255–9.
- [39] Edmunds C, Galloway S, Dixon J, Bukhsh W, Elders I. Hosting capacity assessment of heat pumps and optimised electric vehicle charging on low voltage networks. *Appl Energy* 2021;298:117093, [Online]. Available: <https://www.sciencedirect.com/science/article/pii/S0306261921005420>.
- [40] Wardle R, Davison P. Initial load and generation profiles from CLNR monitoring trials, Durham University, [Online]. Available: <http://www.networkrevolution.co.uk/project-library/initial-load-generation-profiles-clnr-monitoring-trials/>.
- [41] Thormann B, Kienberger T. Estimation of grid reinforcement costs triggered by future grid customers: Influence of the quantification method (scaling vs. Large-scale simulation) and coincidence factors (single vs. Multiple application). *Energies* 2022;15(4), [Online]. Available: <https://www.mdpi.com/1996-1073/15/4/1383>.
- [42] Weiss A, Biedenbach F, Mueller M. Simulation and analysis of future electric mobility load effects in urban distribution grids. In: ETG congress 2021. 2021, p. 1–6.
- [43] Swan LG, Ugursal VI. Modeling of end-use energy consumption in the residential sector: A review of modeling techniques. *Renew Sustain Energy Rev* 2009;13(8):1819–35, [Online]. Available: <https://www.sciencedirect.com/science/article/pii/S1364032108001949>.
- [44] Li Y, O'Neill Z, Zhang L, Chen J, Im P, DeGraw J. Grey-box modeling and application for building energy simulations - A critical review. *Renew Sustain Energy Rev* 2021;146:111174, [Online]. Available: <https://www.sciencedirect.com/science/article/pii/S1364032121004639>.
- [45] Consumption Profiles 2021, mffbas, [Online]. Available: <https://www.mffbas.nl/documenten/>.
- [46] ElaadNL open datasets for electric mobility research, ElaadNL, [Online]. Available: https://platform.elaad.io/analyses/ElaadNL_opendata.php.
- [47] Yu Y, Reihis D, Wagh S, Shekhar A, Stahleder D, Mouli GRC, et al. Data-driven study of low voltage distribution grid behaviour with increasing electric vehicle penetration. *IEEE Access* 2022;10:6053–70.
- [48] Edelstein S. Here's why EVs don't lose as much range in hot-weather AC use. *Green Car Reports*; 2023, https://www.greencarreports.com/news/1140248_here-s-why-evs-don-t-lose-as-much-range-in-hot-weather-a-c-use. [Accessed: 05 August 2023].
- [49] Damianakis N, Mouli GRC, Bauer P. Risk-averse estimation of electric heat pump power consumption. In: 2023 IEEE 17th International Conference on Compatibility, Power Electronics and Power Engineering (CPE-POWERENG). 2023, p. 1–6.
- [50] Smets AH, Jäger K, Isabella O, van Swaaij R, Zeman M. Solar Energy: The physics and engineering of photovoltaic conversion technologies and systems. UIT; 2016.
- [51] Murty P. Chapter 10 - power flow studies. In: Murty P, editor. *Power systems analysis (second edition)*. 2nd ed.. Boston: Butterworth-Heinemann; 2017, p. 205–76, [Online]. Available: <https://www.sciencedirect.com/science/article/pii/B978008101119000100>.